CHAPTER IV
RESULTS AND DISCUSSION

4.1 Asphaltene Precipitation

Figure 4.1 shows the precipitation onset time as a function of heptane concentration for five different crude oils. It can be seen that asphaltene precipitation for these crude oils is a time-dependent process, and onset time exponentially increases by decreasing heptane concentration. This is consistent with previous work (Maqbool *et al.*, 2009).

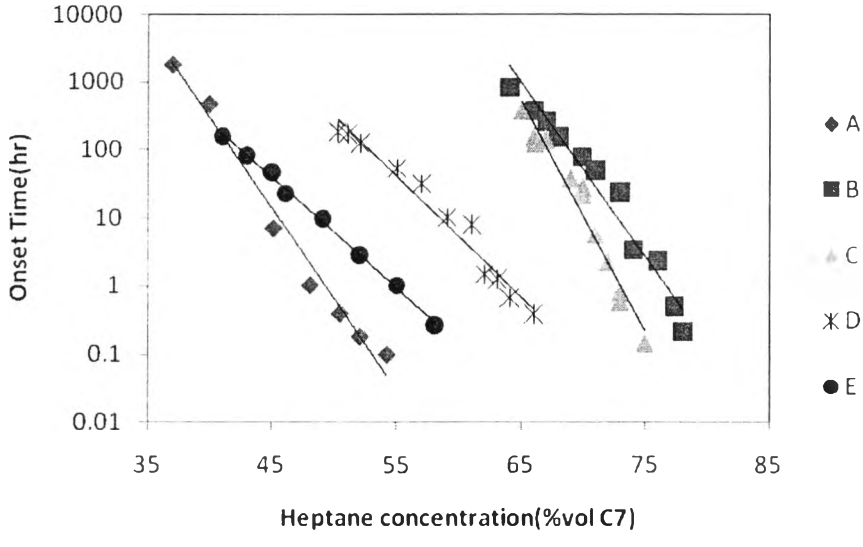

Figure 4.1 Precipitation onset time at varying heptane concentration.

In the oil industry, crude oils are never mixed with a precipitant like n-heptane and the major reason for asphaltene destabilization is due to changes in pressure, temperature and composition (mixing of crude oils). Figure 4.1 shows that asphaltene precipitation for different crude oils is a kinetic process. However, in order to predict precipitation kinetics under field conditions, a better understanding about the factors that control precipitation rates is required. Therefore, our goal in

this work was to describe the precipitation rates with change in mixture properties rather than plotting them as a function of heptane concentration.

Table 4.1 shows the properties of crude oils such as viscosity, refractive index, solubility parameter, density and their asphaltene content.

Table 4.1 The properties of crude oils

Properties	Type of crude oils				
	A	B	C	D	E
Density (g/mL)	0.8698	0.8700	0.9215	0.8523	0.8319
Asphaltene content (% g asphaltenes/g crude oil)	3.2532	0.7434	1.4420	1.4560	0.7810
Refractive index (n)	1.4964	1.4905	1.5204	1.4845	1.4720
Solubility parameter (δ, $MPa^{1/2}$)	18.15	17.99	18.79	17.83	17.49
Viscosity (μ, mPa s)	27.52	19.99	165.78	12.23	5.82

The solubility parameter is used to estimate the degree of interaction between materials (Hansen, 2007). The closer of solubility parameter of asphaltenes to the solubility parameter of solution surrounding them is the higher the stability of asphaltenes. Therefore, to see if the difference observed in precipitation kinetics of different crude oils is dictated by the mixture solubility parameter, the onset times were plotted as a function of mixture solubility parameter (crude oil and heptane) in Figure 4.2. The calculation of solubility parameter of solution is shown in Appendix B.1.

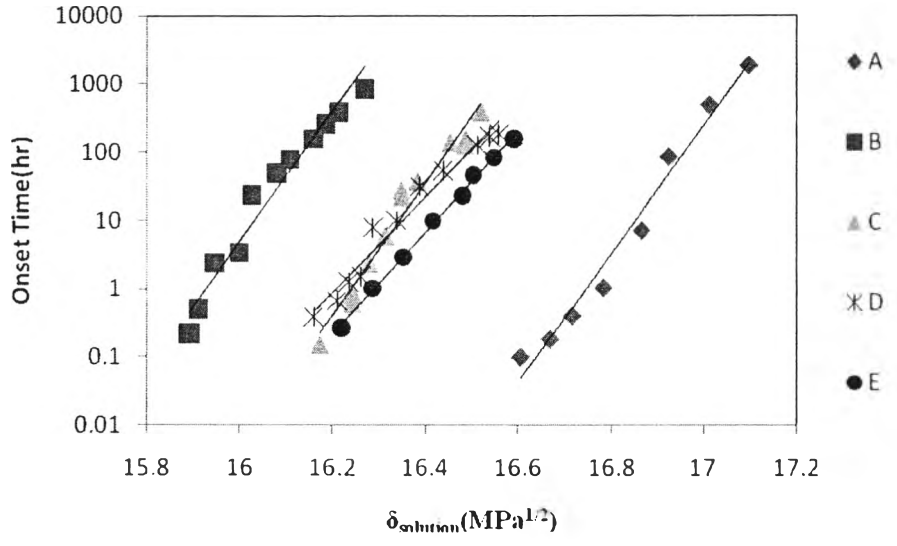

Figure 4.2 Onset time as a function of solubility parameter of solution.

It can be seen that the onset time increases as the solubility parameter of solution increases. Figure 4.2 shows that difference in aggregation rate of asphaltenes is not just due to differences in mixture solubility parameter. Therefore, even though the solubility parameter of solution might have an effect on aggregation rates but it is not the only property responsible for controlling precipitation rate and other properties need to be considered. In all of these five crude oils, not only the solution solubility parameters might be different but also the solubility parameter of asphaltenes in the mixture.

In order to get better understanding about the solubility effect with aggregation rates, a new correlation was developed to account for differences in asphaltene solubility parameters as well of solution solubility parameter. Figure 4.3 shows the correlation between onset time and difference in solubility parameter of asphaltenes and solution. This should give an estimate about the driving force for asphaltenes instability and aggregation. However, because asphaltenes are solid, it is not feasible to directly measure their solubility parameter. Therefore we assumed the solubility parameter of asphaltenes in order to get identical onset times for different

oils. Table 4.2 shows the assumed solubility parameters of asphaltenes for (δ_{asph}- $\delta_{solution}$).

Table 4.2 The assumed solubility parameter of asphaltenes for (δ_{asph}- $\delta_{solution}$)

Crude Oil	Solubility Parameter ($MPa^{1/2}$)
A	22
B	21.2
C	21.5
D	21.55
E	21.6

The onset time increases as the difference between solubility parameter of asphaltenes and solution decreases for every crude oil. When solubility parameters of asphaltenes are close to solubility parameter of solution, asphaltenes are soluble and completely disperse in the solution. It can be seen that the trend and slope of this correlation are similar for every crude oil (Figure 4.3). Therefore the interaction forces between asphaltenes are a driving force that control aggregation process.

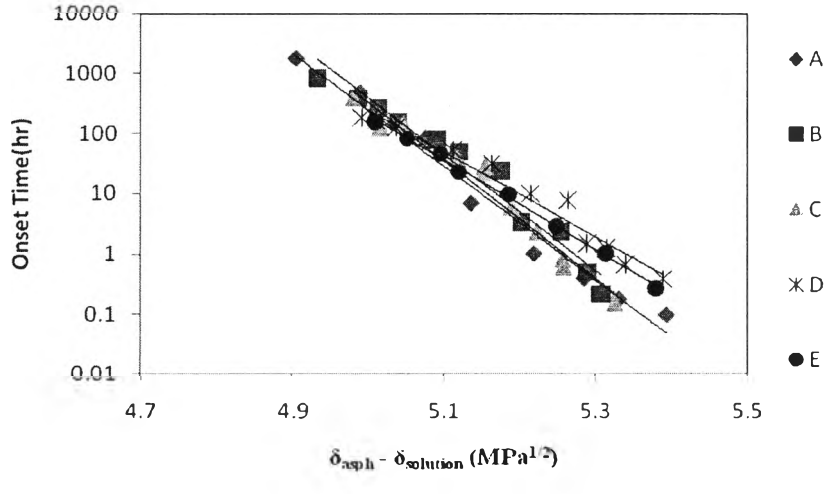

Figure 4.3 The relationship between onset time and $\delta_{asph} - \delta_{solution}$.

Even though the difference in solubility parameter of asphaltenes and solution provides an estimate about driving force required for aggregation process but it does not provide any information about diffusion rate of asphaltenes. The viscosity of solution can be used to explain the diffusion process of asphaltenes in solution. In order to get information regarding diffusion rate of asphaltenes with aggregation rates, the inverse viscosity was used. Therefore, the relationship between onset time and inverse viscosity of solution were plotted as shown in Figure 4.4. The viscosity of solution was calculated from viscosity of each component as shown in Appendix B.2. The onset time increases as the viscosity of solution increases. It is harder for asphaltenes to diffuse and collide with each other in solutions with higher viscosity and this leads to decrease in their aggregation rate.

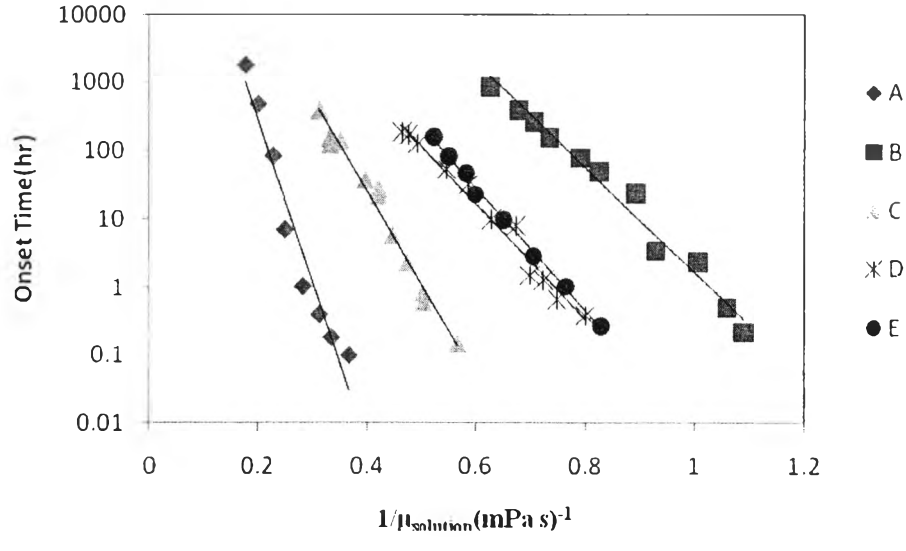

Figure 4.4 Precipitation onset time with viscosity of solution.

In order to have thermodynamics and transport properties in the same correlation, the combination of all properties discussed earlier needs to be considered. The solubility parameters of asphaltenes were assumed to get identical onset time for different crude oils as shown in Table 4.3. Therefore, all physical properties were plotted as a function of onset time as shown in Figure 4.5. The onset

time decreases as the x-axis variable, $((\delta_{asph}- \delta_{solution})^2/\mu_{solution})$, decreases. This correlation can be explained in every crude oil because the trend and slopes are the same. Therefore, the precipitation rates of asphaltenes are controlled by solubility parameter of asphaltenes, solubility parameter of solution and viscosity of solution. The relationship is shown in Eq (4.1).

Table 4.3 The assumed solubility parameter of asphaltenes for $(\delta_{asph}- \delta_{solution})^2/\mu_{solution}$

Crude Oil	Solubility Parameter ($MPa^{1/2}$)
A	24.2
B	19.9
C	22.1
D	21.1
E	21.2

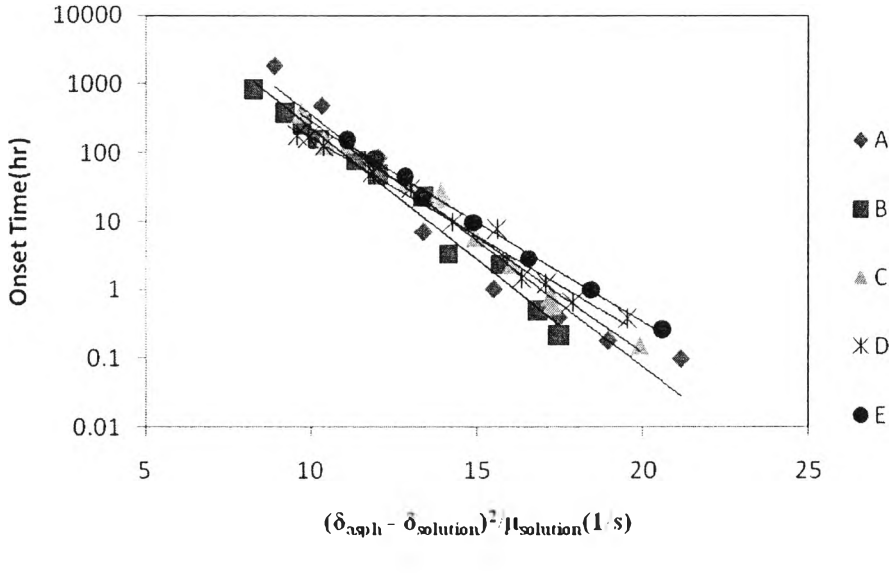

Figure 4.5 The onset time vs $(\delta_{asph} - \delta_{solution})^2/\mu_{solution}$.

$$Asphaltene precipitation \quad \alpha \quad \frac{(\delta_{asphaltene} - \delta_{solution})^2}{\mu_{solution}} \qquad (4.1)$$

4.2 Amount of Precipitated Asphaltenes

The centrifugation technique developed by Maqbool (2011) was used to study the amount of asphaltene precipitated as a function of time and precipitant concentration. Amount of precipitated asphaltenes increases as a function of time and heptane volume fraction, a result consistent with previous work (Figure 4.6). Asphaltenes are assumed that they are destabilized instantaneously after heptane is added. Then the destabilized asphaltenes collide and form larger aggregates. The destabilized asphaltenes are separated out by the centrifugation technique when it is bigger than minimum diameter. The minimum diameter of particle that can be separated using the centrifugation technique can be calculated if knowing solution properties are known (Appendix A.1).

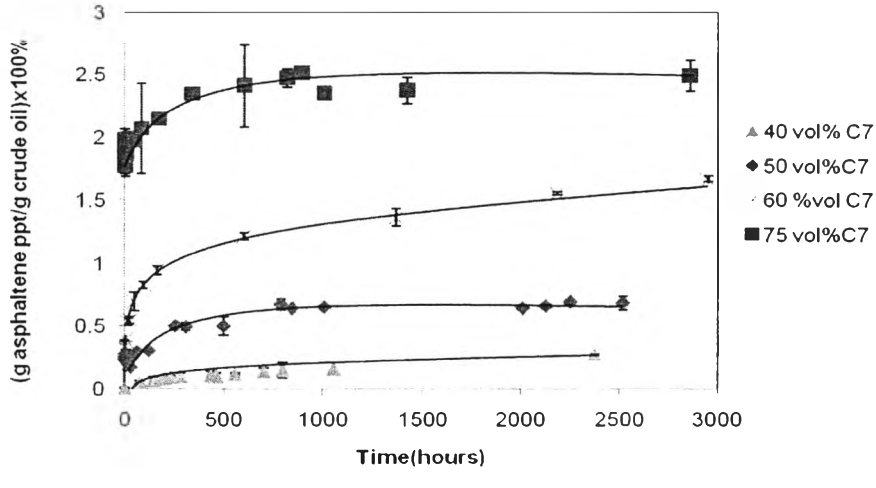

Figure 4.6 Centrifugation plot at different heptane concentration.

Centrifugation results were used as a guideline to determine the fractionation times for 50 vol% and 75 vol% heptane as can be seen from Figure 4.7 (a) and 4.7 (b). For 50 vol% heptane in crude oil, the entire solution was centrifuged

at 4 hours (*Cut 1*), 76 hours (*Cut 2*), 837 hours (*Cut 3*) and 2257 hours (*Cut 4*). *Cut 1* includes the asphaltenes precipitated in the first four hours. *Cut 2*, *Cut 3* and *Cut 4* include the asphaltenes precipitated from 4 to 76 hours, 76 to 837 hours and 837 to 2257 hours. For 75 vol% heptane, the solution was centrifuged at 4 hours (*Cut 6*) and 1100 hours (*Cut 7*). *Cut 6* and *Cut 7* include the asphaltenes precipitated in first four hours and from 4 to 1100 hours.

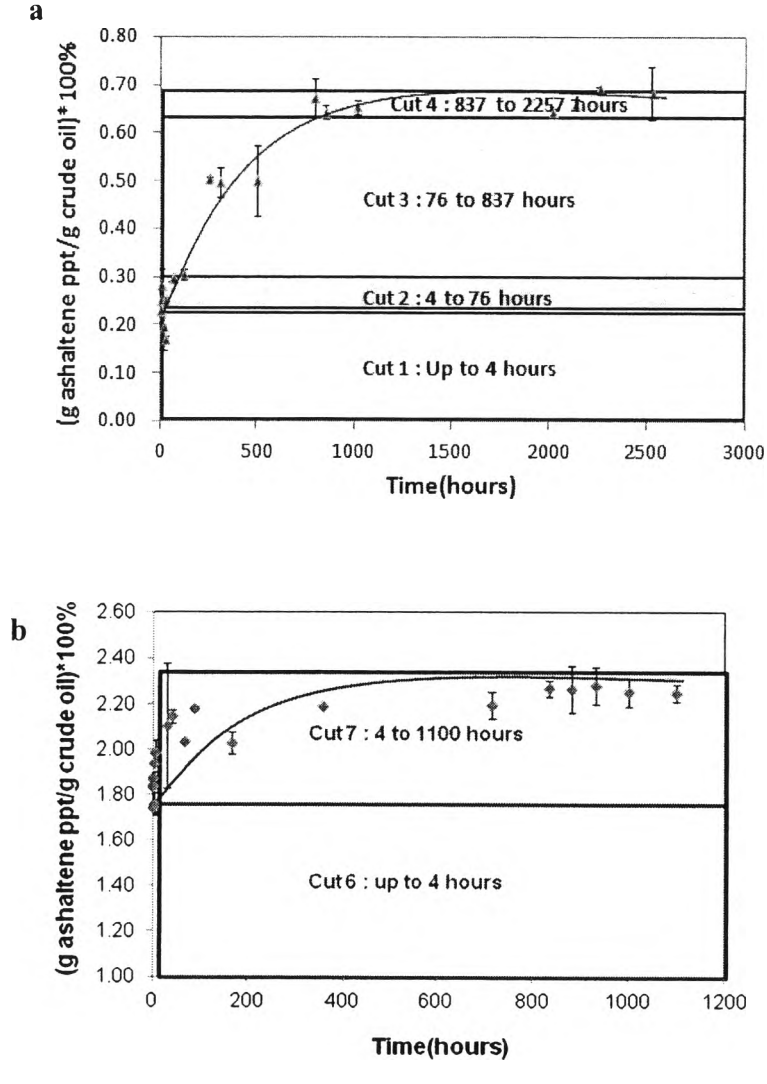

Figure 4.7 Centrifugation plot for different cut at same heptene concentration (a) 50 vol% heptane. (b) 75 vol% heptane.

4.3 Characterization of Asphaltenes as a Function of Time and Precipitant Concentration

The onset plot and yield of precipitated asphaltenes showed that asphaltenes precipitation had different behavior at different times and precipitant concentrations. There are two possible reasons for asphaltenes that precipitated at different condition: either asphaltenes need time to grow up or the different in properties of asphaltenes. Therefore, this study measured the properties of asphaltenes at different time and precipitant concentration.

4.3.1 Solubility of Asphaltenes

Total asphaltenes and asphaltenes collected at different times and heptane concentrations were dissolved in toluene and observed under optical microscopy. Figure 4.8 shows that all cuts except *cut 1* were completely soluble in toluene. A fraction of *cut 1* was insoluble in toluene even after one week and two hours of sonication. Table 4.4 shows the amount of soluble and insoluble fraction for *cut 1* asphaltenes in toluene. It shows that the soluble fraction of asphaltenes for *cut 1* is around 51 wt% (Appendix C). Similar behaviour was observed when *cut 1* was dissolved in chloroform, dimethylene chloride and tetrahydrofuran. *Cut 1* was not completely soluble in these solvents although they are believed to be good solvents for asphaltenes. Therefore, the insoluble part might not be asphaltenes. They might be waxes, sand, or other solid particles.

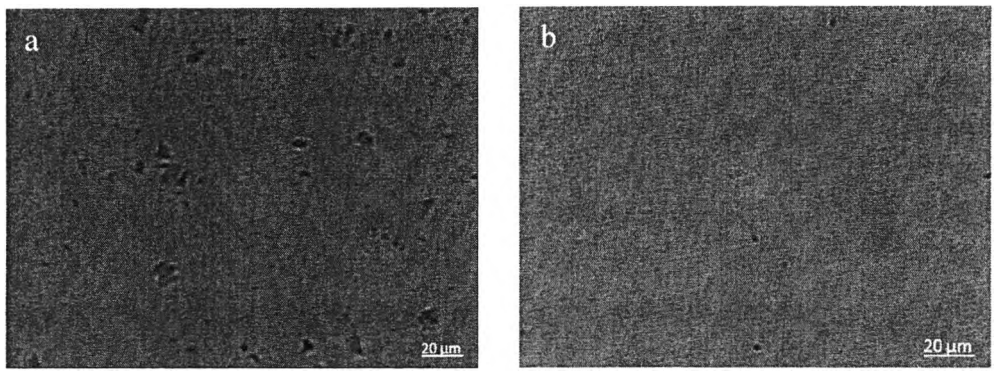

Figure 4.8 Asphaltene particles in toluene by using optical microscopy (a) *Cut 1* and (b) Other cuts of asphaltenes.

Table 4.4 Soluble and insoluble asphaltenes for *cut 1* in toluene

Fraction of soluble asphaltenes	0.5141
Fraction of insoluble asphaltenes	0.4859

4.3.2 Cut 1

The solubility results showed that *cut 1* was not completely soluble in toluene, chloroform, dichloromethane and tetrahydrofuran, although these solvents are believed to be good solvents for asphaltenes. Therefore, one might think that insoluble fractions of *cut one* are not asphaltenes and are some other compounds like waxes, sand or solid particles from crude oil. In order to investigate the possibility of the insoluble compounds being wax, some extra analyses were done on insoluble fraction of *cut 1*. Waxes are alkyl chain hydrocarbons that are soluble in solvents like toluene or heptane at high temperatures.

4.3.2.1 High Temperature Experiments for Cut 1 in Toluene

Cut 1 was dissolved in toluene and then heated. The solution was observed under optical microscopy. Solubility of asphaltenes and waxes increases by temperature. Therefore, if the insoluble particles are gone after heating, there is the possibility that they are waxes and not sand particles since the solubility of sand particles does not increase with this amount of heating. Figure 4.9 shows the

microscopy pictures of *cut 1* in toluene at room and elevated temperature (75 °C). The insoluble particles disappear at 75 °C. There are two possible explanations for this result. First, insoluble particles might be asphaltenes that have better solubility at high temperature. Second, they might be waxes.

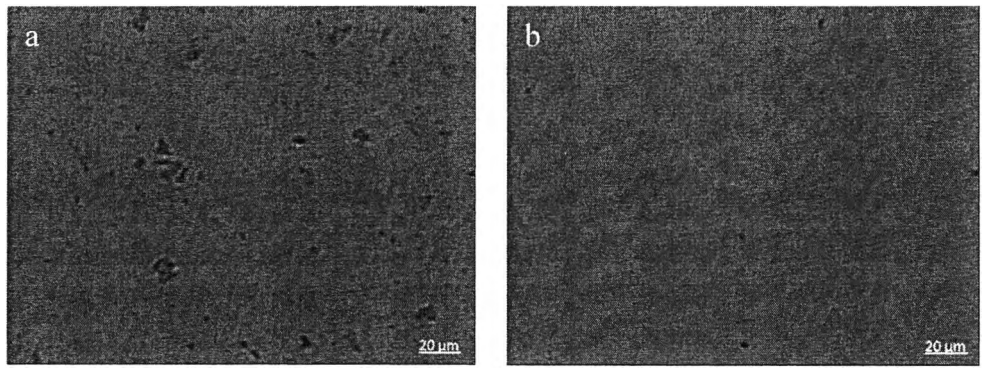

Figure 4.9 The microscopy pictures of *cut 1* in toluene (a) 20 °C (b) 75 °C.

4.3.2.2 High Temperature Experiments for Insoluble Cut 1 in Heptane

In order to see whether the insoluble fraction of *cut 1* comprises asphaltenes or waxes, high temperature experiments were conducted in heptane. The insoluble fractions are likely waxes if they are soluble in heptane at elevated temperatures. However, they are more likely asphaltenes if they remain insoluble even at high temperature in heptane (heptane is a precipitant for asphaltenes). Figure 4.10 shows optical microscopy pictures of insoluble particles of *cut 1* in heptane at room temperature (20 °C) and 85 °C. The insoluble particles decreased in number as the temperature was increased. However, they never completely disappeared, even though the temperature was increased up to 85 °C. The insoluble particles in heptane are asphaltenes and the soluble particles in heptane consist of waxes.

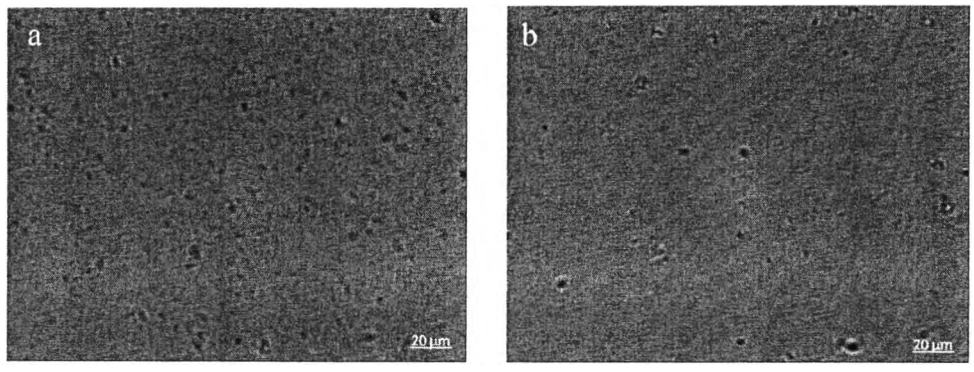

Figure 4.10 Insoluble particles of *cut 1* in heptane (a) room temperature (20 °C) (b) 85 °C.

4.3.2.3 Asphaltenes Stabilization

Solubility results showed that *cut 1* was not soluble in toluene, chloroform, dimethylene chloride, and tetrahydrofuran. Although total asphaltenes also include *cut 1*, they were completely soluble in toluene. Total asphaltenes consist of *cut 1*, *cut 2*, *cut 3* and soluble asphaltenes for 50 vol% of heptane in crude oil as shown in Figure 4.11 (a). If *cut 1* is soluble in toluene after it is mixed with other cuts, it demonstrates that *cut 1* is asphaltenes that can be stabilized by other asphaltenes. Therefore, *cut 1*, *cut 2*, *cut 3* and soluble asphaltenes for 50 vol% heptane were mixed together in toluene based on weight fraction of each cut in total asphaltenes as shown in Figure 4.11 (b) (Appendix D).

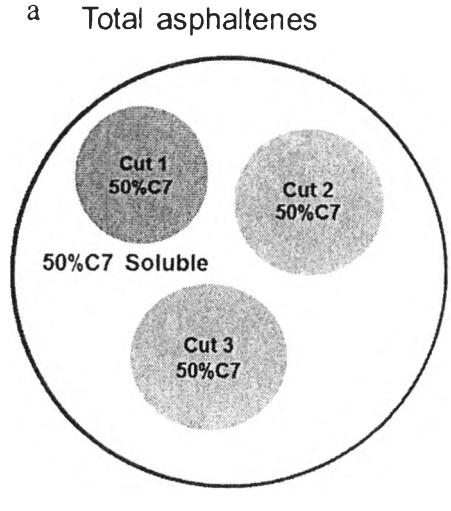

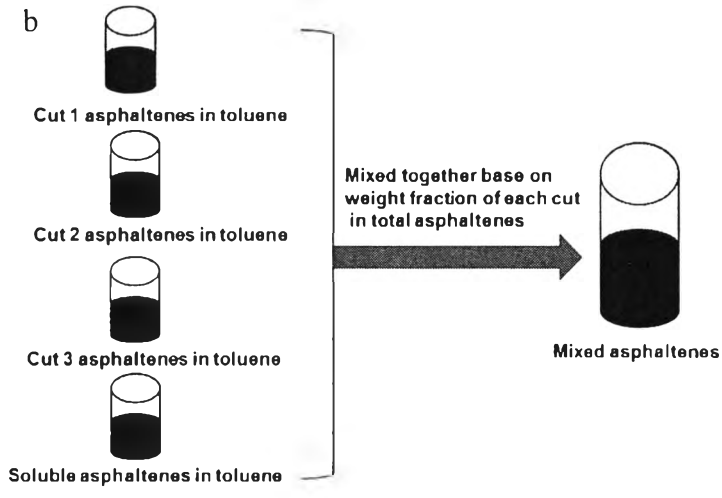

Figure 4.11 (a) Composition of total asphaltenes (b) Schematic of mixed asphaltenes experiment.

The mixed asphaltenes in toluene were observed under optical microscopy. Figure 4.12 shows mixed asphaltenes were completely soluble in toluene similar to total asphaltenes. The soluble fraction stabilizes the insoluble fraction (*cut 1*) and helps them to dissolve in solvent, consistent with Spiecker *et al.* (2003)'s results, which showed that the soluble fraction can self-stabilize the precipitated fraction to dissolve in toluene.

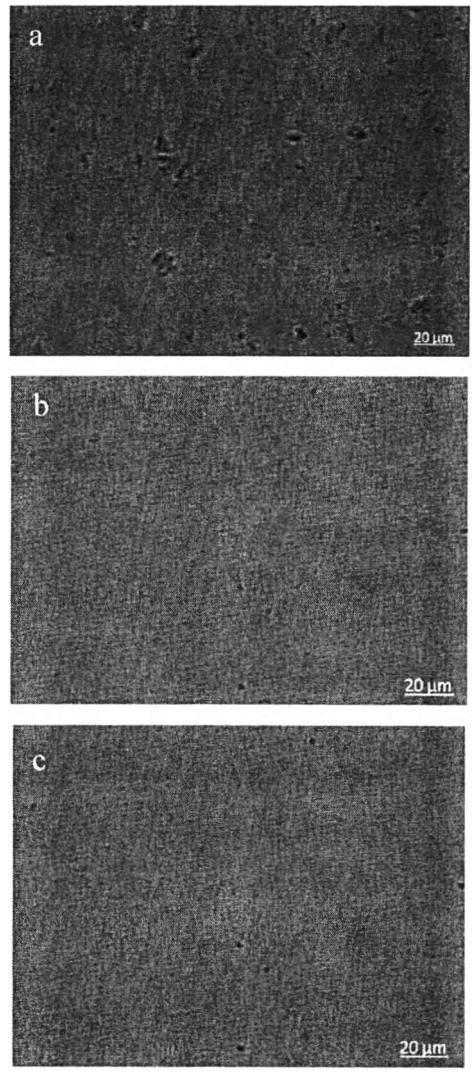

Figure 4.12 Asphaltene particles in toluene by using optical microscopy (a) *Cut 1* (b) Mixed asphaltenes (c) Total asphaltenes.

Mixed asphaltenes were also analysed using SAXS. The scattering result of mixed asphaltenes and total asphaltenes in Figure 4.13 are identical, agreeing with particle size of nanoaggregates in Table 4.5. The particle sizes of nanoaggregates were analyzed using Guinier Approximation. It shows that stable asphaltenes stabilize the unstable fraction in toluene and reduce their sizes consistent with solubility results.

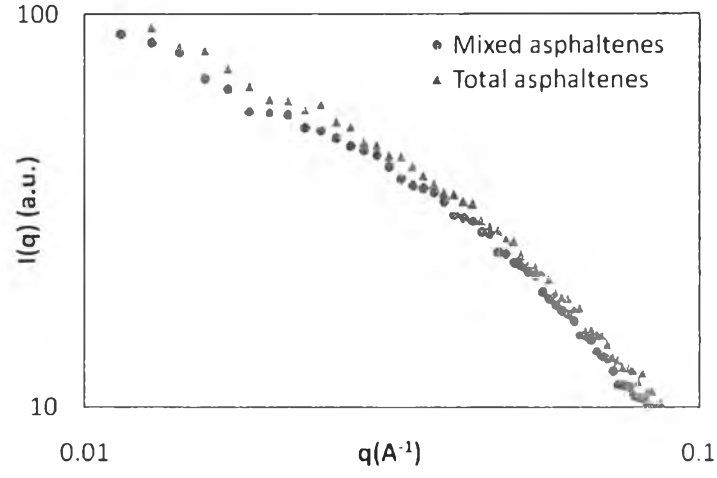

Figure 4.13 The relationship between q and intensity of scattering of mixed and total asphaltenes.

Table 4.5 Particle size of nanoaggregates

Type of asphaltenes	Particle size(nm)
Total asphaltenes	8.14 ± 0.59
Mixed asphaltenes	8.06 ± 0.64

Therefore, there was small fraction of *cut 1* that was mixed with other asphaltenes in toluene (Appendix D). The self-stabilization of asphaltenes in these results is possibly from dilution of *cut 1* in solution. The dilution of *cut 1* might make it hard to observe insoluble particles under optical microscopy.

4.3.2.4 Mix Cut 1 with Soluble Asphaltenes

The *cut 1* was mixed with soluble asphaltenes for 75 vol% heptane in order to make sure that stabilization effects observed in previous section were not just due to dilution. In order to compare this experiment with a previous experiment (*Cut 1* in toluene or Section 4.3.1), *cut 1* was prepared base on similar fraction with toluene experiment. Therefore, 2 wt% of *cut 1* was mixed with 2 wt% of *soluble asphaltenes for 75 vol% heptane* to measure the insoluble fraction of *cut 1*.

If the *soluble asphaltenes for 75 vol% heptane* stabilize *cut 1*, the insoluble fraction should decrease. The optical microscopy pictures of *cut 1*, *soluble asphaltenes for 75 vol% heptane*, and the two cuts mixed together are shown in Figure 4.14. The insoluble particles in *cut 1* were decreased after they were mixed with soluble asphaltenes. Therefore, some of insoluble particles are stabilized by soluble asphaltenes.

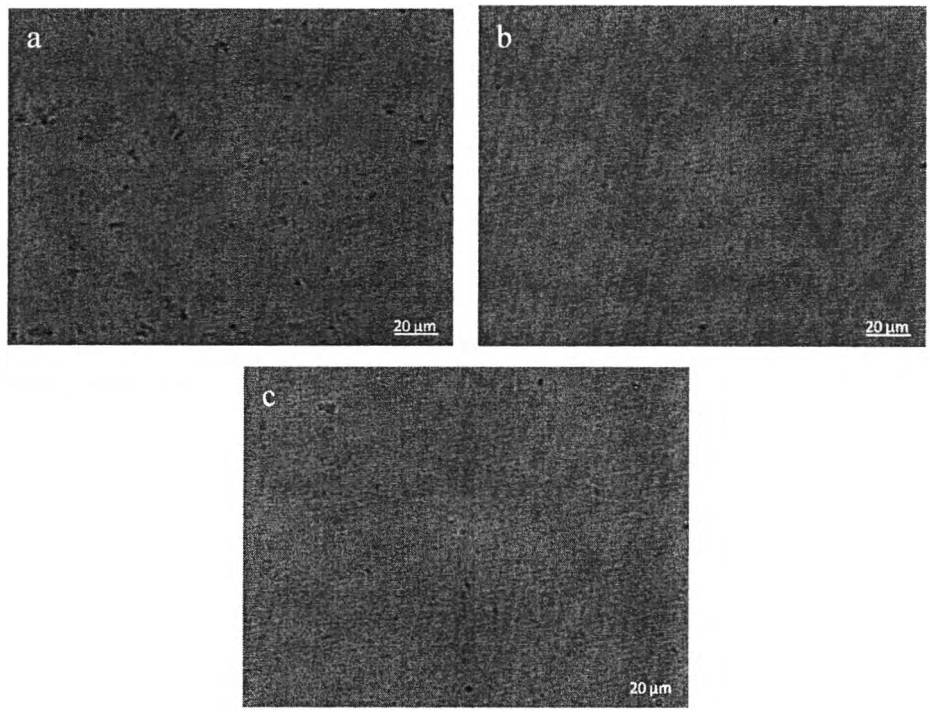

Figure 4.14 Optical microscopy pictures (a) 2 wt% of *cut 1* in toluene (b) 2 wt% of *75 vol% heptane soluble asphaltenes* in toluene (c) mix *cut 1* and *75 vol% heptane soluble asphaltenes* in toluene.

The insoluble fraction of *cut 1* before and after mixing with soluble asphaltenes is shown in Table 4.6.

Table 4.6 Fraction of insoluble particles of *cut 1* before and after mixing with *soluble asphaltenes for 75 vol% heptane*

Mixed with soluble asphatenes	Fraction of insoluble particles	Wt% of insoluble paticles in toluene
Before	0.4859	1.02
After	0.1263	0.53

The insoluble fraction decreased after *cut 1* was mixed with *soluble asphaltenes*. This demonstrated that half of insoluble particles in *cut 1* are probably asphaltenes because they are stabilized by soluble asphaltenes (Table 4.5). The other portion of the insoluble particles might be waxes because it disappears when heated in toluene and heptane.

4.3.3 Small Angle X-Ray Scattering (SAXS)

Asphaltenes that precipitated at different times and precipitant concentrations were dissolved in toluene (1 wt% in toluene) and analysed using small angle X-ray scattering (SAXS). As mentioned earlier, *cut 1* was not completely soluble in toluene. Therefore, *cut 1* was centrifuged at 14000 rpm for 10 minutes to separate out insoluble fraction. The soluble solution after centrifugation was analyzed using SAXS. Figure 4.15 shows the comparison between scattering vector (q) and intensity (I(q)) for precipitated, soluble and total asphaltenes. The Guinier Approximation can be used to obtain a shape-independent estimate of the radius of gyration of asphaltene particles (Appendix E).

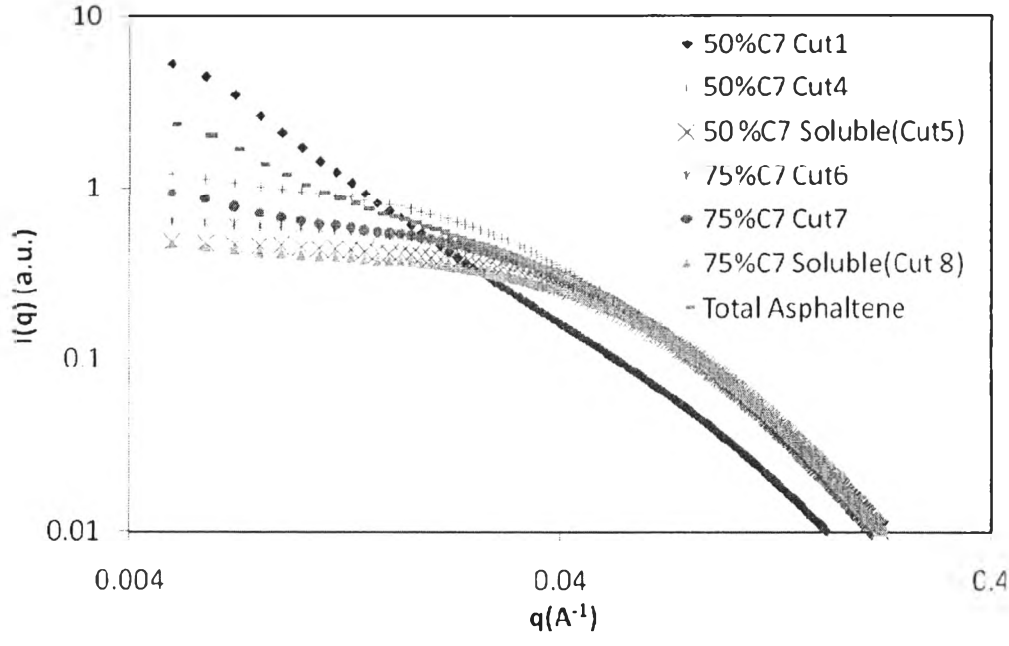

Figure 4.15 The relationship between q and intensity of scattering for each cut and total asphaltenes.

The results were used to estimate the size of nanoaggregates by applying Guinier Approximation at low q :

$$\ln(I) = \ln(I_0) - \left(\frac{R_g^2 q^2}{3}\right) \qquad (4.2)$$

The slope and intercept of data were then used to calculate $-\frac{R_g^2}{3}$ and $In(I_0)$, respectively (Appendix E). The radiuses of gyration (R_g) for precipitated, soluble and total asphaltenes are shown in Table 4.7. Scattering results show that *cut 1* had sharp upturn, therefore Guinier Approximation cannot be used to estimate size of particles. The particle size of total asphaltenes was estimated using middle q range because there was upturn at low q likely due to the effect of cut 1 particles.

Table 4.7 The gyration radius of aggregated asphaltenes

concentration		R_g(nm)
50 vol% C7	*Cut 1*	-
	Cut 4	5.15 ± 0.15
	Soluble (*Cut 5*)	3.14 ± 0.05
75 vol% C7	*Cut 6*	3.79 ± 0.07
	Cut 7	3.70 ± 0.06
	Soluble (*Cut 8*)	2.82 ± 0.03
Total		6.42 ± 0.43

Table 4.7 shows soluble asphaltenes are smaller than precipitated asphaltenes in each concentration. Moreover, the particle sizes of nanoaggregates in each cut are close to each other but *cut 1* particles are too large to be characterized by SAXS. C*ut 1* contained asphaltenes and waxes (Section 4.3.2), and therefore the large particle size of nanoaggregate for *cut 1* might be the effect of waxes. In other cuts besides *cut 1*, asphaltenes that precipitated earlier are more unstable and they have higher possibility to succeed when they collide other destabilized asphaltenes and become bigger.

4.3.4 Heteroatoms and Metal Contents

Table 4.8 shows the carbon, hydrogen, heteroatoms (N, O and S) and metal contents (Ni and V) for different cuts.

Table 4.8 Heteroatoms and metal contents

Type of asphaltenes	%wt						Ni	V
	C	H	N	O	S	H/C	(ppm)	(ppm)
50 vol% C7 *Cut 1*	82.86	11.12	0.55	2.7	4.33	1.61	88	237
50 vol% C7 Cut 3	80.9	7.48	1.15	2.17	7.7	1.11	172	537
50 vol% C7 *Cut 4*	81.41	7.35	1.11	2.79	7.6	1.08	160	495
50 vol% C7 soluble (*Cut 5*)	81.18	7.81	1.02	1.82	7.26	1.15	139	442
75 vol% C7 *Cut 6*	81.27	7.77	1.07	2.13	7.48	1.15	148	453
75 vol% C7 *Cut 7*	80.61	7.56	0.98	1.94	7.36	1.13	142	424
75 vol% C7 soluble (*Cut 8*)	81.07	7.79	1.01	3.79	7.06	1.15	129	394
Total asphaltenes	81.5	7.79	1.05	2.21	7.2	1.15	152	479

The heteroatom and metal contents of different cuts were plotted in Figures 4.16 and 4.17, respectively.

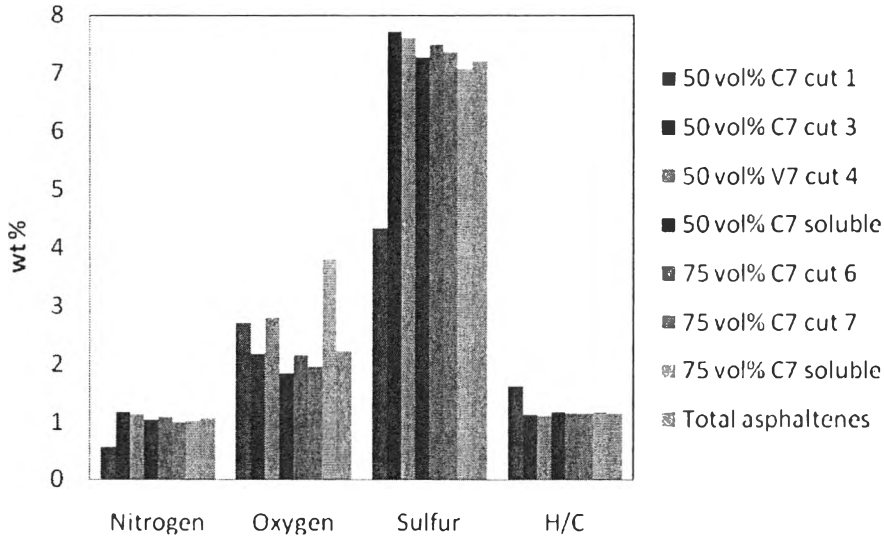

Figure 4.16 Heteroatom contents and hydrogen per carbon ratio for different cuts.

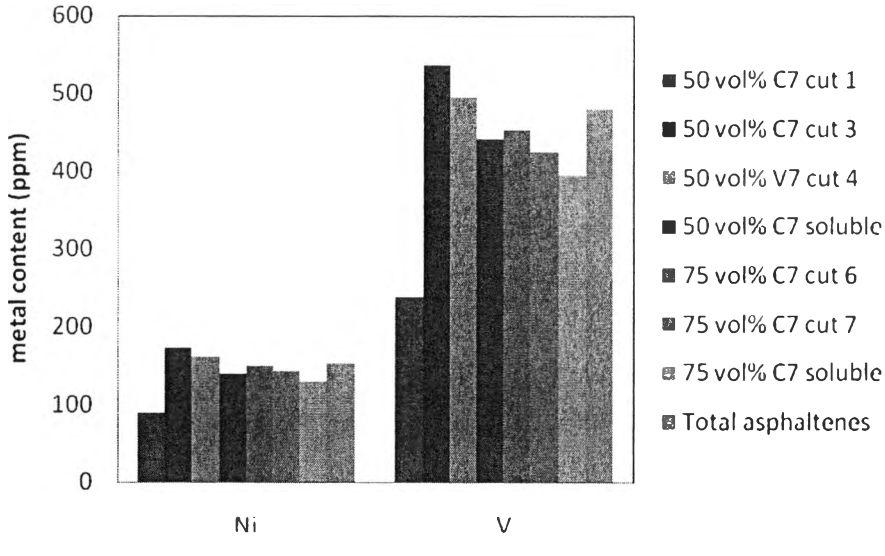

Figure 4.17 Metal contents for different cuts.

In all cuts except for *cut 1*, asphaltenes had higher heteroatoms and metal contents in each concentration for the asphaltenes precipitated at earlier times. However, there was not a significant difference between H/C ratio for different cuts. If asphaltenes had high heteroatom and metal contents, they had higher polar fraction.

Since high polar fraction causes asphaltenes to precipitate more easily, it makes sense that asphaltenes with high heteroatom and metal contents precipitate more easily. These results supported the results of SAXS that showed asphaltenes precipitated at earlier times and formed larger nanoaggregates. *Cut 1* had the highest H/C ratio and the least heteroatoms and metal contents. As mentioned earlier (Section 4.3.2), *cut 1* contained asphaltenes and waxes. Therefore, *cut 1* had the highest H/C ratio because some of *cut 1* were waxes. This supported the experiment of *cut 1* in previous section.

4.3.5 Nuclear Magnetic Resonance (NMR)

The structure parameters such as aromaticity and number of carbons per alkyl side chain are shown in Table 4.9.

Table 4.9 Structure parameters of asphaltenes

Type of asphaltenes	H_γ	H_β	H_α	H_{ar}	n	C_{ar}	C_{al}	f_a
50 vol% heptane								
- *Cut 1*	1.00	3.86	1.33	0.62	4.65	0.18	1.00	0.15
- *Cut 1 soluble*	1.00	3.80	1.24	0.65	4.87	0.26	1.00	0.21
- *Cut 2*	0.15	0.45	0.20	0.1	4.00	0.24	0.74	0.25
- *Cut 3*	0.15	0.47	0.20	0.1	4.10	0.26	0.73	0.26
75 vol% heptane								
- Soluble (*Cut 8*)	1.00	3.70	1.36	0.68	4.46	0.34	1.00	0.25
Total	1.00	3.21	1.31	0.72	4.21	0.35	1.00	0.26

Asphaltenes that precipitated in different conditions had similar aromaticity except for *cut 1*. The number of carbons per alkyl side chain (n) increased as a function of times and precipitant concentrations. The longer alkyl side chain (higher n) makes aromatic cores of asphaltenes hard to collide with each other.

Cut 1 had higher number of carbons per alkyl side chain (n), with long alkyl side chains that prevented aggregation. *Cut 1* also has less interaction forces to

aggregate due to lowest aromiticity supported the result of heteroatom (Section 4.3.4). These results demonstrated that *cut 1* contained waxes, supporting the previous results. Although *cut 1* was centrifuged and the soluble solution of *cut 1* was analyzed using NMR, it still had low aromaticity and high number of carbons per alkyl side chain. It showed that waxes cannot be separated using the centrifugation technique at room temperature.

The properties of asphaltenes that precipitated at different times and precipitant concentrations were not identical. The asphaltenes that precipitated earlier, except *cut 1*, had higher heteroatom and metal contents and lower numbers of carbons per alkyl side chain. There were similar particle sizes of nanoaggregates and aromaticity of asphaltenes at different conditions. This demonstrated that the higher in heteroatom and metal contents lead asphaltenes easily to aggregate due to the polar fraction. The shorter length of alkyl side chain (lower number of carbon per alkyl side chain) makes it easier for aromatic cores to get closer. Hence there is higher possibility that leads asphaltenes to collide and form larger nanoaggregates.